# PHY324 - Interferometer Report

Chaitanya Kumar Mahajan & Meet Chaudhari

December 29, 2023

**Abstract**

This report summarizes the usage of interference patterns of monochromatic and white light sources produced in a Michelson interferometer to calculate the index of refraction of a thin microscope glass plate and air. To make accurate measurements, the calibration factor of $-0.197 \pm 0.002$ was found to relate the actual movement of an end mirror in the interferometer with the reading on the micrometer screw. Using white light fringes, the refractive index of thin microscope glass plate was calculated as $1.56 \pm 0.01$ which is near the accepted value of 1.5. Similarly, by counting circular fringes of monochromatic light of Sodium lamp, the refractive index of air was calculated as $1.000 \pm 0.009$ which is within one deviation of the accepted value of 1.0036.

# 1 Introduction[1]

An interferometer is a device that employs the fact that electromagnetic waves add with each other or interfere to create an interference pattern of bright and dark fringes. A common type of interferometer is the Michelson interferometer which divides a beam of light into two daughter light beams of equal amplitude which are then sent along its two perpendicular directions to get reflected back and interfere with each other. A typical Michelson interferometer has a wide range of applications which include measuring structure of spectral lines, refraction indexes of materials, and determining the speed of light in perpendicular directions. We used such an interferometer to find the refractive indices of a thin microscope glass plate and air at standard temperature.

## 1.1 General Setup

The standard apparatus set up used for Michelson interferometer is shown in figure 1. It involves a light source whose light enters the interferometer through a diffusion screen. This screen diffuses the source's light so that the source effectively becomes an extended object emitting light. The light goes through a beam splitter (G1) which reflects 50% of the beam in the vertical direction towards $A_1$ via the reflecting surface (R) at the back of the beam splitter while the other 50% is transmitted through it along the horizontal arm towards mirror $A_2$. These are then reflected from the end mirrors and recombine at G1. The interference fringe pattern then depends on the the path length differences that the *light travels* in each arm (shown as $d$ in figure 1). Note that the beam travelling in the vertical direction crosses the width of the G1 three times however, the beam travelling along the horizontal arm crosses the width of the G1 twice. To compensate for this difference a compensation plate of the same material and thickness is added in the horizontal path so that the light travels the necessary extra width. Therefore, to change the effective path length difference one can either change position of mirror $A_1$ or introduce a different medium in the path of one of the arms. Also, the mirror $A_2$'s inclination could be changed to observe different kinds of interference fringes.

## 1.2 Interference patterns and theory

When the interference pattern is observed, they are seeing 2 virtual images of the source from the mirrors $A_1$ and $A_2$ which basically act as two separate light sources. The light beam from each of these "sources" are in phase as the path length difference zero. The interference pattern produced by the Michelson interferometer consists of circular fringes (see figure A.6) when the

[1]All information is this subsection is summarized from PHY324 Interferometer Lab Manual. https://www.physics.utoronto.ca/ phy224_324/experiments/interferometers/INTERFER.pdf

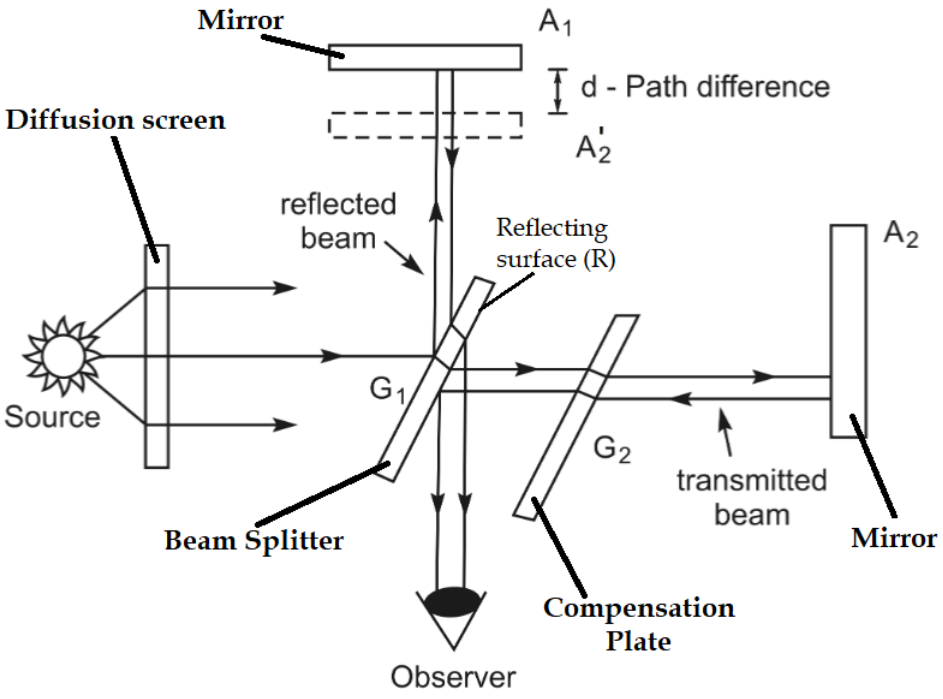


Figure 1: *General setup of the Michelson interferometer. Light from source is split into two perpendicular directions at G1. Reflected beam is reflected of mirror A1 while transmitted beam is reflected at mirror A2. Both beams recombine at G1 and is observed. G2 is needed to ensure that there is no extra path length due to reflections inside the G1 mirror. Mirror A1 is movable and controls the path difference while mirror A2's orientation can be controlled to ensure A1, A2 are perpendicular. Figure edited from PHY324 Interferometer Lab Manual*

two mirrors $A_1$ and $A_2$ are perpendicular with respect to each other. This means that the virtual images overlap exactly. Since the mirrors and hence the virtual images are circular, we can define a perpendicular axis connecting the observer and the centre of the virtual images. Now, observing a particular point at an angle $\theta$ with respect to this axis on the circular images, the path length difference between the light rays coming from each coherent source for maxima and minima is:

$$2d\cos\theta = m\lambda \tag{1}$$

where $d$ is the distance difference between the two mirrors from the centre of beam splitter(see figure 1), $\lambda$ is the wavelength of light under consideration, and $m$ is the fringe order. Since the angle $\theta$ remains constant along a circle centred at the centre of the virtual images, light received from these points will be in phase with each other. This leads to observation of circular fringes. When observing the fringe at the centre, we have $\theta = 0$. Since the interference pattern shrinks and expands as we move past the zero path length difference point, we get that at the centre, using equation 1:

$$m = \frac{2d}{\lambda} \tag{2}$$

This means that one fringe disappears in the centre exactly when the mirror $A_1$ is displaced by a distance $d$. This is important in finding the calibration factor to relate the distance the mirror $A_1$ moves when the micrometer screw's reading is changed as this will cause fringes to disappear in the centre. Thus, we can find $f$ such that:

$$d = M \cdot f \tag{3}$$

where $M$ is the distance the micrometer is moved and $d$ is the actual distance by which the mirror $A_1$ is displaced by.

One can also observe localized fringes which appear when the two mirrors are not exactly perpendicular (see figure A.7). This is accomplished by tilting the mirror $A_2$ with respect to the mirror $A_1$. The localised fringes are exactly vertical at the position of zero path length difference because it means small sections of very large concentric circular fringes are being observed. Using this, we can also observe white light fringes (see figure A.8) which only occur in a very narrow range around the zero path length difference of monochromatic light.

If a micrometer slide of thickness $t$ and an index of refraction $\mu$ is inserted in one of the beam paths in the interferometer, then the path length difference becomes

$$2t(\mu - 1) = m\lambda = d \tag{4}$$

Simplifying, we get an explicit prediction of the refractive index of the microscope slide using equations (3, 2):

$$\mu = \frac{Mf}{t} + 1 \tag{5}$$

Lastly, using the same procedure but with monochromatic light, we can also calculate the refractive index of air at standard temperature and pressure. This is measured by using the fact the refractive index of a gas depends on the pressure and density of a gas. Using these facts, the index of refraction of the gas could be calculated as:

$$n_0 = 1 + \frac{dN}{dP}\frac{\lambda}{2l}\frac{760T}{273} \tag{6}$$

where $n_0$ is the index of refraction of air, $N$ is the number of fringes, $P$ is the pressure of air, $\lambda$ is the wavelength of monochromatic light, and $T$ is the temperature of the air. Therefore, one can insert a container of air in one of the beam paths and measure the rate at which circular interference fringes disappear with respect to changes in the pressure of air inside. This can be used in conjunction with equation 6 to measure the index of refraction.

## 1.3 Materials & Apparatus

To conduct the experiment, we used a Michelson Interferometer (see figure A.4) where the micrometer has an uncertainty of $\pm 0.01$ mm. For monochromatic light source, we used a Sodium lamp ($\lambda = 589.3 \pm 0.1$nm) and used a bulb emitting white light as a source of white light. We used a Vernier caliper with accuracy $\pm 0.02$ mm to measure lengths of different components. For measuring refractive index of a solid, we used a microscope glass slide of thickness $0.98 \pm 0.02$ mm and two slide holders. For measuring the refractive index of air, we used a hollow gas cell with circular glass walls of width $5.00 \pm 0.02$ mm, cavity length $50.71 \pm 0.02$ mm, and a stand to attach it to optical bench. Three reinforced plastic tubes were connected to it to a vacuum pump. Another compensation plate consisting of 2 similar glass plates each of width $5.00 \pm 0.02$ mm with the total width being $11.70 \pm 0.02$ mm (due to casing) was used to correct for the presence of glass lids in the air cell. Finally, the required Edward High Vacuum Ltd. rotary vacuum pressure pump system for connecting to the gas cell. It had a dial gauge indicating pressure range of $1 - 760$ mm Hg with least count 20 mm Hg and uncertainty in measurement of $\pm 10$ mm Hg due to dial fluctuations. It also included a small fine adjustment release valve, and a main access valve.

# 2 Procedure

**Calibration:** It is necessary to find a calibration factor $f$ to relate the micrometer position and the actual lateral displacement of $A_1$ as in equation 3. To do this, we made a standard setup of the Michelson interferometer as seen in figure A.4. Then, using a Sodium lamp (due to the large range of path length difference) we allowed the monochromatic light to enter the interferometer via a diffusion screen. Observing the virtual images of the light source from each mirror through the viewing hole and align the images by adjusting mirror $A_2$ using its side knobs to tilt it such that its virtual image coincided with that of mirror $A_1$. This meant that the mirrors were perpendicular to each other. By trial and error, we moved the carriage attached with mirror $A_1$ to be able to see concentric circular fringes in the field of view as seen in figure A.6 with a bright fringe in the middle. We recorded this initial micrometer reading and put a smartphone at the observer position with its camera zoomed in at the centre of the interference pattern. This was done for the ease of observing the fringes[2].

Since we could either create fringes or destroy them in the centre of field of view, we decided to destroy them because it's clear when a fringe disappears in the middle. We then slowly moved the mirror $A_1$ carriage towards us by rotating the micrometer screw and recorded the micrometer reading after fifty fringes had disappeared up to a total of a thousand fringes. We had to rotate it slowly to count the fringes and tried to cause minimum disturbance to the optical bench to reduce random fringe movement. We also ensured that the micrometer dial was slowly turned because an overshoot was not easily corrected by turning the dial backward. The complete data-set is shown in table 1

**Index of Refraction of Solid:** We use white light fringes as their appearance is very sensitive to small path length differences which is ideal since the glass slide has small thickness. Since these fringes occur at zero path length difference, we generated vertical local fringes by adjusting mirror $A_2$'s orientation (one knob will control the curvature while the other controls the rotation of the fringes) and the position of mirror $A_1$'s carriage. This created larger separation between the local fringes as seen in A.7 from which it was less unambiguous whether the fringes were vertical or had a curvature. Once a good fringe spacing is reached, we switched to a white light and slowly turned the micrometer screw to locate the white light fringes (this occurs over a very small range, so it is best to try turning the screw in both directions over a small range.) Figure A.8 shows the white light fringes that can be observed. We recorded the micrometer reading and placed a microscope slide between mirror $A_1$ and beam splitter. We ensured that the slide was entirely parallel to mirror $A_1$ by adjusting the slide holder. Then, we rotated the mirror $A_1$'s micrometer screw slowly to relocate the white-light fringes and note the new micrometer reading. Finally, we measured the glass thickness with a Vernier caliper and used the calibration factor from the previous measurement and equation 5 to calculate the index of refraction of the slide.

**Index of Refraction of Gas:** We first measure the air cavity length excluding the top caps and glass. Since we compensate for the extra glass by adding an identical glass in $A_2$ path. Then, we fixed the gas cell between the beam splitter and mirror $A_1$ (see figure A.5) on the optical bench by tightening the nuts. We then turned on the vacuum pump and decided to increase pressure from $50 \pm 10$ Hg mm to $700 \pm 10$ Hg mm because it led to destruction of fringes which was easier to count. Then, we again used a smartphone to observe the fringe pattern in the centre. By using the main access valve for major pressure changes and the pressure release

[2]By observing with naked eyes and through the smart phone camera, we confirmed that it was able to identify the bright and dark fringes correctly.

valve for smaller increments in the pressure, we noted the pressure readings for destroying one fringe at a time starting from a bright fringe. In the whole process, we made sure to keep the vacuum pump separate from the optical bench to isolate its vibrations. The data-set for this experiment is shown in table 2.

# 3 Results & Discussion

**Calibration:**
We measured the micrometer position and the number of fringes that disappear. By equation 2, where $\lambda = 589.3 \pm 0.1$nm (uncertainty chosen as $\pm$ one unit of last significant figure, as the actual sodium lamp did not report any uncertainty) is the mean sodium spectral wavelength, we convert the fringe count data to lateral carriage movement. In figure 2 we plot the carriage distance in mm vs the micrometer position in mm with uncertainties derived from least count of micrometer screw. The line of best fit $y = (-0.197 \pm 0.002) \cdot x + (3.28 \pm 0.02)$ mm is also plotted which was optimized via `scipy.optimize.curve_fit`. Then, according to equation 3, the calibration factor $f$ is the slope of the curve:

$$f = -0.197 \pm 0.002 \text{ AU}$$

Notice that the reduced $\chi^2$ value is 0.22 and the corresponding p-value is 1.0. This may suggest an over-fitting of the fitting curve and the data, however due to the nature of the data (low relative uncertainty) and its visible linearity, a high p-value is expected. This also suggests that the mirror $A_1$ micrometer knob linearly displaces mirror $A_1$, i.e. for any unit change in the micrometer, we expect a uniform unit change in the lateral displacement, leading us to conclude that the screw threads are uniform.

**Index of Refraction of Solid:**
Very vertical local fringes for sodium light source were observed at a micrometer reading of $10.37 \pm 0.01$ mm. After changing the light source to a white light, local white light fringes were observed at $10.31 \pm 0.01$ mm. Then, inserting a microscope slide and ensuring it was parallel to mirror $A_1$, we observed white light fringes at $13.08 \pm 0.01$ mm. However, the white light fringes were not entirely vertical, leading us to conclude that the glass slide was not entirely parallel (we moved around the slide in multiple orientations and angles, but never generated entirely vertical fringes). The glass thickness was measured to be $t = 0.98 \pm 0.02$ mm. By equation 5 and using the calibration factor $f$ and thickness $t$ we found that,

$$\mu = 1.53 \pm 0.01 \text{ AU}$$

The theoretical index of refraction of a microscope slide is 1.50 AU[3]. However this value depends on the thickness and exact chemical composition of the slide. As a rough estimate, the calculated value of the index of refraction is within $3\sigma$ of the theoretical accepted refraction index of glass.

**Index of Refraction of Air:**
The gas cell cavity was measured to be $50.71 \pm 0.02$ mm long without including the glass walls. We tried to reduce uncertainties, but the vacuum pump engine fumes were released close to the interferometer setup, potentially changing the path-length of the light outside the gas cell because it would change the index of refraction of air outside the gas cell randomly. The air temperature was $(22 \pm 1)^o$C and we assume the air temperature in the gas cell was the same

[3]PHY324 Interferometer Lab Manual

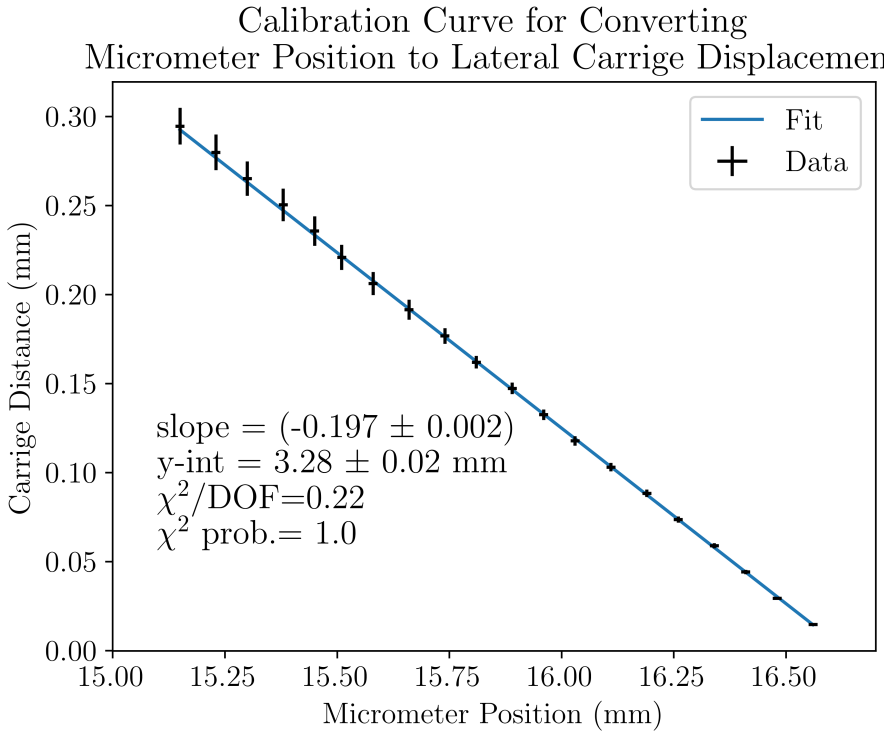


(a) *Plot of data and best fit line of mirror $A_1$ carriage displacement vs the micrometer position. The fringe count was converted to lateral displacement via $d = \frac{m\lambda}{2}$ and a best fit curve for the relationship was found as $y = (-0.197 \pm 0.002) \cdot x + (3.28 \pm 0.02)$ mm. The $\chi^2_{red} = 0.22$ and associated probability of 1.0 are expected due to the clear relationship. Full calibration data found in appendix, table 1.*

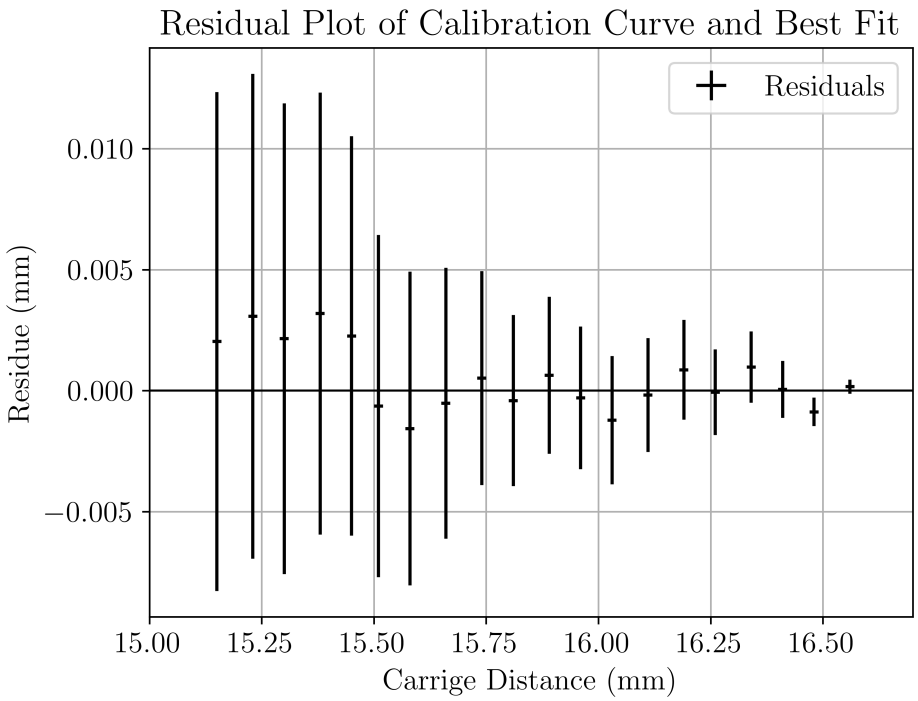


(b) Residual plot between the measured carriage distance and the fit values from $y = (-0.197 \pm 0.002) \cdot x + (3.28 \pm 0.02)$ mm. Notice that every value is either at 0 or its uncertainty range contains 0 which means the fit is a very good one.

Figure 2: *Calibration curve and residual plots for the lateral displacement of mirror $A_1$ and micrometer position.*

and did not change throughout the experiment because we conducted the experiment fairly quickly.

In Figure 3, we plotted the pressure in the gas cell per fringe that disappeared. Along with the data we also plot the optimized curve $y = (15.5 \pm 0.1)$ mm Hg $x + (51 \pm 3)$ mm Hg where the optimal parameters were found using the *curve_fit* function. The reduced $\chi^2$ is 0.36 and the corresponding p-value is 1.0. As before, this large p-value is expected since the data is largely uniform and linear and very slight deviation from the optimal fit as seen in the residual plot in subfigure (b) in figure 3 .

The rate of change of fringe per pressure is then,

$$\frac{dN}{dP} = \frac{1}{15.5 \pm 0.1} \text{ fringe/(mm Hg)} \approx 0.0645 \pm 0.0004 \text{ fringe/(mm Hg)}$$

By equation 6, the index of refraction of air was calculated to be,

$$n_0 = 1.000306 \pm 0.000002 \text{ AU}$$

The accepted refraction index of air is, $n_0^{\text{accepted}} = 1.000277$ AU and so $n_0/n_0^{\text{accepted}} = 0.99997 \pm (2 \cdot 10^{-6})$ AU which leads us to conclude the presence of some systematic error in our measurements. This can be atttributed to the presence of fumes emitted by the vacuum pump as well as a slight difference in the temperature inside the cavity as these will change the composition of air in the path of the light beams thus altering the effective refractive index of air.

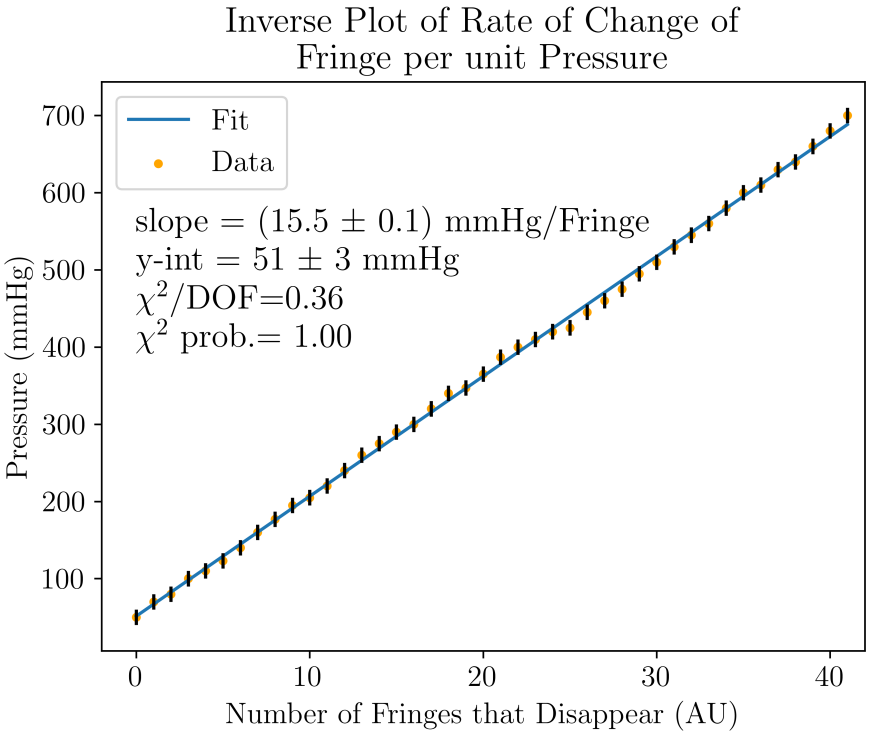


(a) *Plot of data and best fit line of change in air cavity pressure per concentric circular fringe that disappears in the centre of the field of view in a Michelson interferometer to calculate the refractive index of air at standard temperature. Complete data-set found in Appendix. 2*

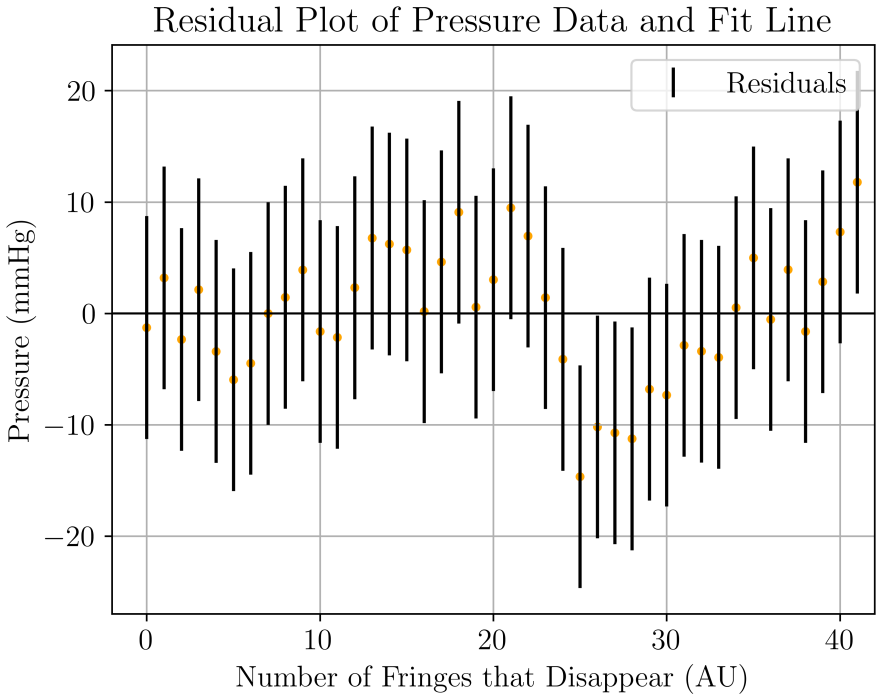


(a) *Residual plot between the measured pressure change per disappearing fringe and the fit values in a Michelson interferometer to measure the refractive index of air at standard temperature. Notice that although the residual varies, every value is either at 0 or its uncertainty range contains 0.*

Figure 3: *Plot of the rate of change of pressure in the glass cell per fringe that disappears, the best fit line, and the corresponding residual plot. These were plotted to derive the refractive index of gas at standard temperature which was found as* $1.000306 \pm 0.000002$ *AU which is ideal because speed of light in air is almost equal to that in vacuum.*

# 4 Conclusion

In this experiment, we calculated the refractive indices of a thin microscope slide and that of air at standard temperature-pressure by using the Michelson interferometer to observe disappearance of interference fringes with Sodium lamp light and light from a white bulb.. The refractive index of glass slide was found as $1.53 \pm 0.01$ AU which is within $3\sigma$ of accepted value of 1.50 AU. The refraction index of air was found as $1.000306 \pm 0.000002$ AU which differed from the accepted value of 1.000277 AU due to the presence of systematic errors like gas fumes from the vacuum pump.

To relate end mirror displacement with the micrometer screw reading and aid in the above measurements, the calibration factor of $-0.197 \pm 0.002$ AU was found by fitting data of mirror movement with the micrometer reading with a fit quality of $\chi^2_{red} = 0.22$ and probability of it being a good fit as 1.0. Overall, the results were very accurate and precise relative to the standard accepted values.

# A Images & Data Tables

| Uncertainty in Every Group of 50 Fringes | Micrometer Position (±0.01 mm) | Uncertainty in Every Group of 50 Fringes | Micrometer Position (±0.01 mm) |
|---|---|---|---|
| 1 | 16.56 | 1 | 15.81 |
| 1 | 16.48 | 3 | 15.74 |
| 2 | 16.41 | 4 | 15.66 |
| 1 | 16.34 | 3 | 15.58 |
| 1 | 16.26 | 2 | 15.51 |
| 1 | 16.19 | 4 | 15.45 |
| 1 | 16.11 | 3 | 15.38 |
| 1 | 16.03 | 2 | 15.30 |
| 1 | 15.96 | 1 | 15.23 |
| 1 | 15.89 | 1 | 15.15 |

Table 1: Micrometer position at every 50 fringes that disappear starting at $16.63 \pm 0.01$ mm up to a total of 1000 fringes. The uncertainty in the fringe count comes from random vibrations which make the fringe count unclear and/or from miscounts of fringes.

| Pressure/fringe destroyed (±10mmHg) | Pressure/fringe destroyed (±10 mmHg) | Pressure/fringe destroyed (±10 mmHg) | Pressure/fringe destroyed (±10 mmHg) | Pressure/fringe destroyed (±10 mmHg) |
|---|---|---|---|---|
| 50 | 205 | 365 | 510 | 680 |
| 70 | 220 | 387 | 530 | 700 |
| 80 | 240 | 400 | 545 | |
| 100 | 260 | 410 | 560 | |
| 110 | 275 | 420 | 580 | |
| 123 | 290 | 425 | 600 | |
| 140 | 300 | 445 | 610 | |
| 160 | 320 | 460 | 630 | |
| 177 | 340 | 475 | 640 | |
| 195 | 347 | 495 | 660 | |

Table 2: Pressure in the air cavity starting at 50 mmHg and working up to 700 mmHg. Uncertainty in the pressure values comes from the gauge reading being unclear as it would fluctuate significantly.

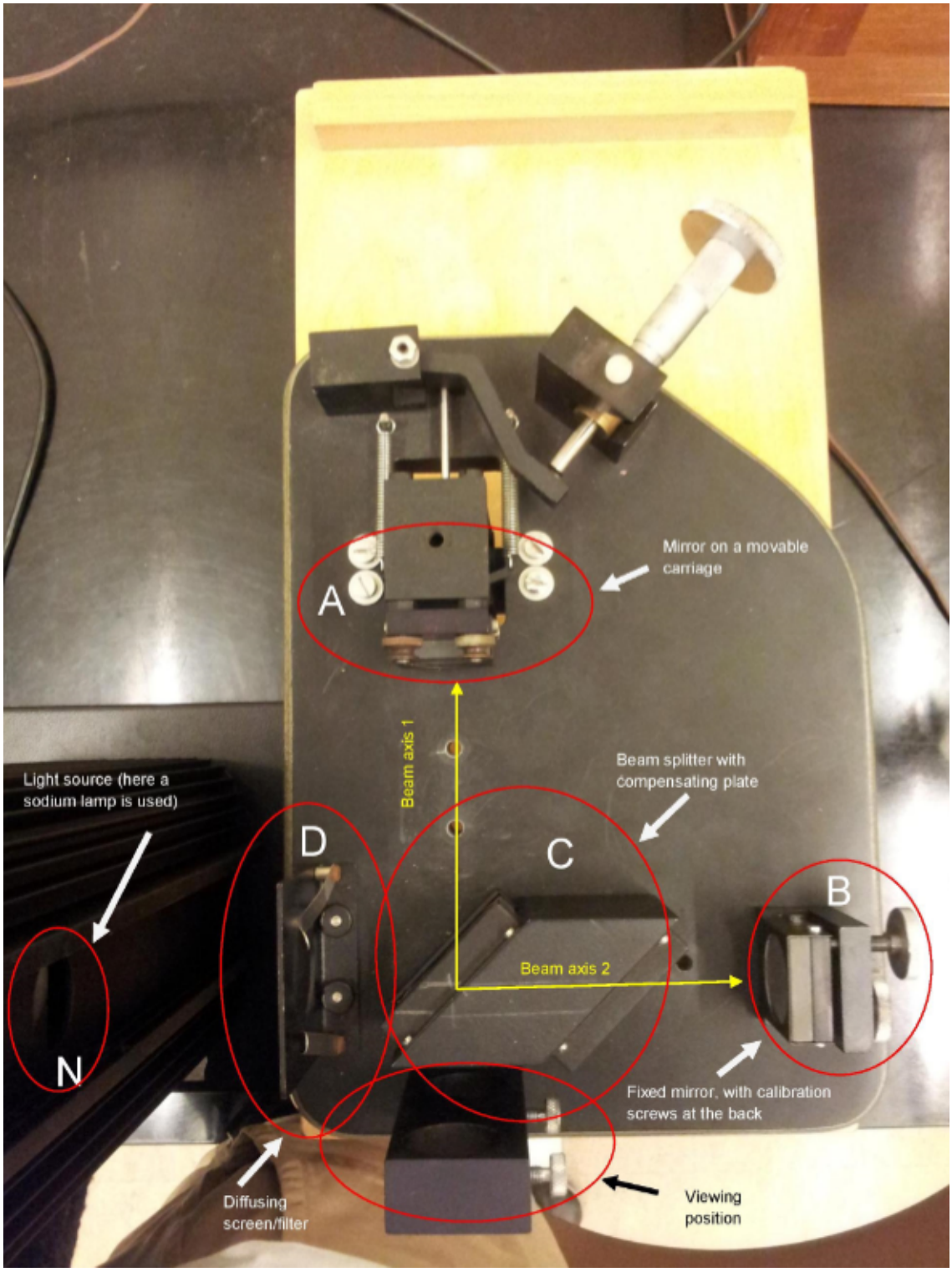


Figure A.4: *From PHY324 Interferometer Manual.* A is the movable mirror where its lateral motion is controlled by the micrometer dial at the top right. B is the second mirror, where its orientation is controlled by the two knobs on the side. C is the beam splitter and D is the diffusion screen. N is the light source (Sodium light (monochromatic) or white-light). Bottom piece is the viewing hole.

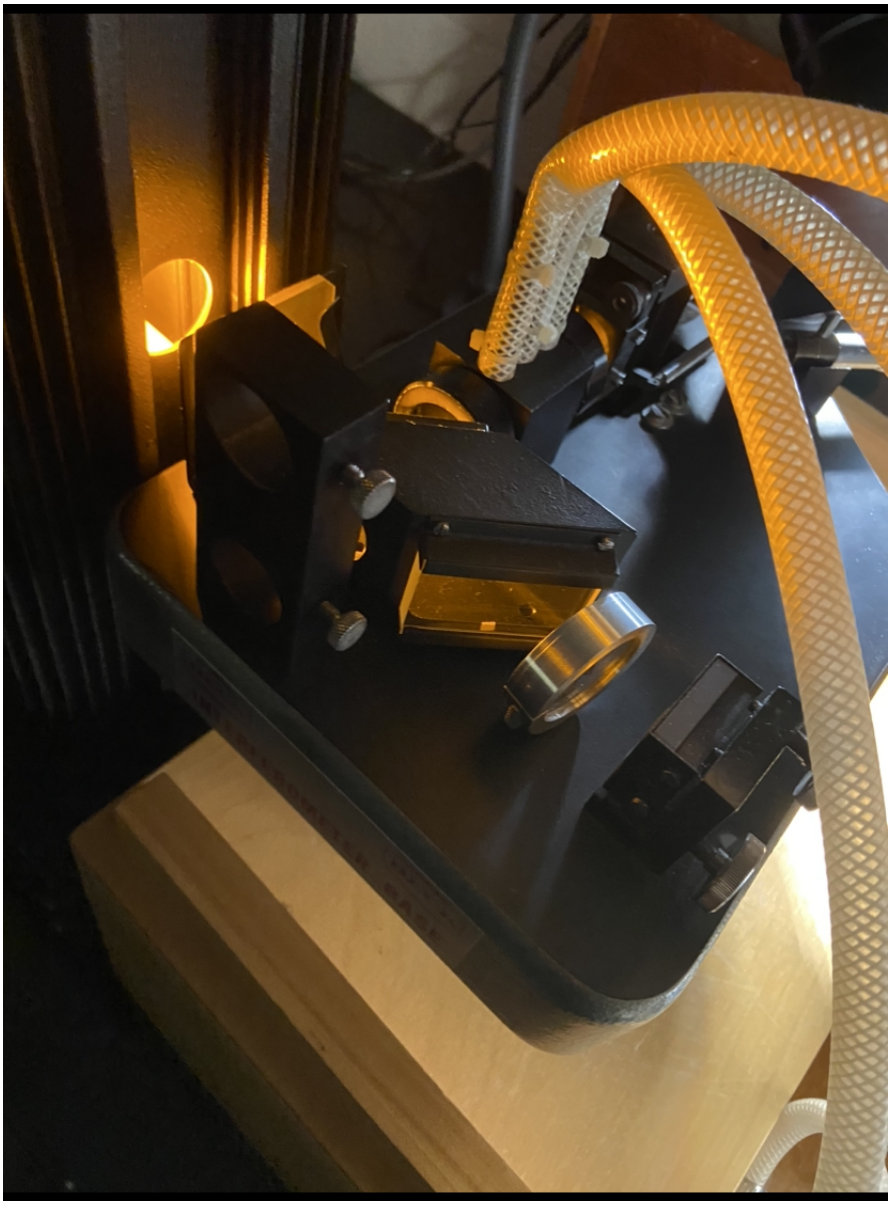

Figure A.5: Setup for measuring refractive index of air

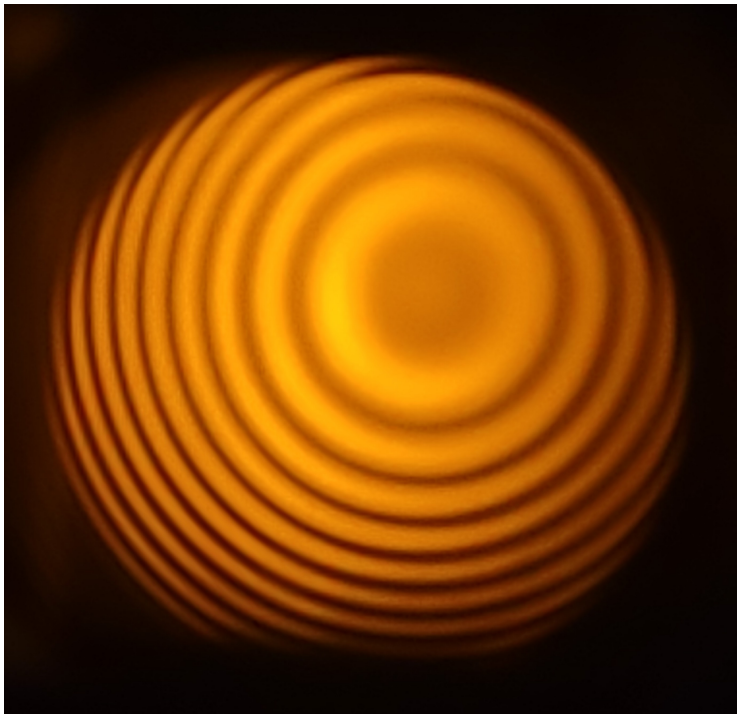

Figure A.6: Circular fringes produced from monochromatic Sodium light source. Fringes appear non-centered due to angle at which the image was taken.

Figure A.7: Local fringes produced from monochromatic Sodium light source.

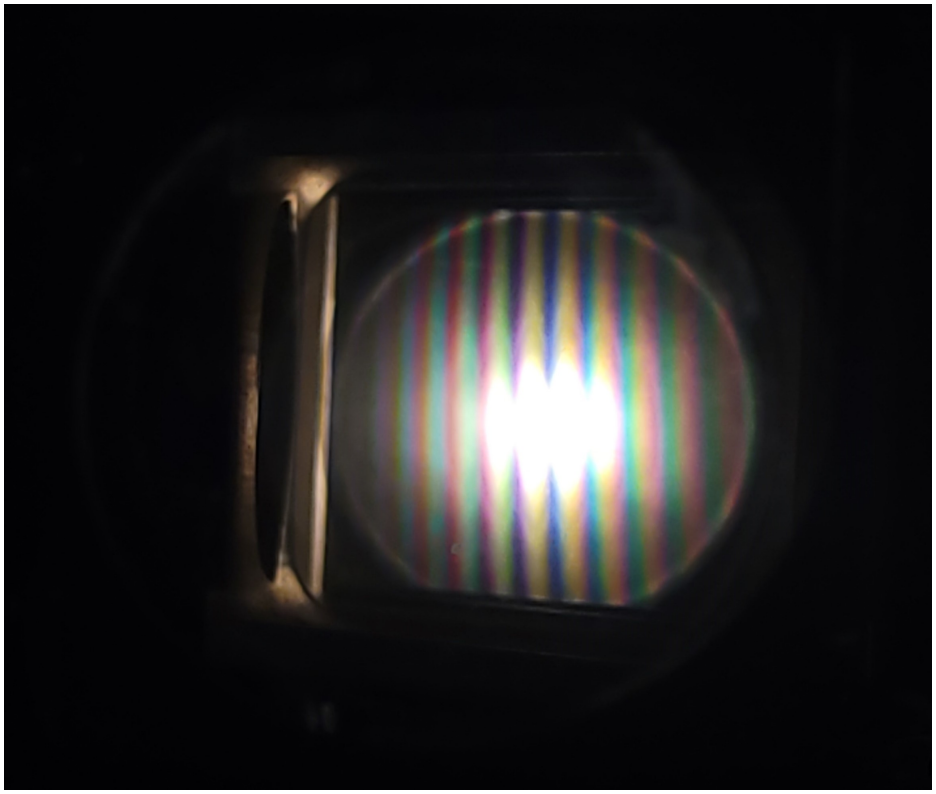

Figure A.8: White light fringes produced from using a white-light for the light source in A.4.

# References

1. PHY324 Instructors. (n.d.). PHY324 Interferometer Lab Manual.
In https://www.physics.utoronto.ca/ phy224_324/experiments/interferometers/INTERFER.pdf.
Physics Department.